Statistical Correlation Between First and Second-Order PMD

E. Ibragimov, *Member, IEEE*, G. Shtengel, *Member, IEEE*, and S. Suh, *Member, IEEE*

***Abstract*—We investigate the statistical correlation between first- and second-order polarization mode dispersion (PMD) effects, which is important for PMD mitigation. The theoretical results are compared to numerical simulations and experimental data from a real high-PMD fiber. A new dependence between first- and second-order PMD is found. We show that the root mean square (rms) value of the second-order PMD component, perpendicular to PMD vector, increases with the length of the PMD vector.**

***Index Terms*—Optical components, optical fiber communications, optical fiber theory, polarization, signal reconstruction, transmission lines.**

I. Introduction

ONE of the difficulties in compensating polarization mode dispersion (PMD) is caused by its statistical nature. In order to compensate PMD, it is essential to know the statistical characteristics of the different PMD parameters. Such considerations must include not only first-order PMD but also higher order of PMD. Much of this information is now available. Statistics characterization, including probability density functions (pdfs) of second-order PMD (SOPMD), is given in [1], [2]. It was previously noticed that the SOPMD vector and the PMD vector are not statistically independent but tend to be perpendicular to each other [1]. It is also known that the PMD vector and the component of the SOPMD vector parallel to it are statistically independent [2]. However, the statistical dependence between first- and second-order PMD vectors has not yet been fully investigated. An important question is: provided a known value of the differential group delay (DGD) in the line, what is the probability of finding a certain value of the magnitude of SOPMD? In other words, what is the conditional probability of SOPMD, assuming that the DGD has a certain value? This problem appeared while testing a YAFO PMD compensator using a 12-stage automatic PMD emulator. When testing a behavior of the compensator, what kind of second-order and higher order PMD should one test with the given value of DGD? Does the SOPMD increase when the DGD goes up, or does it decrease? Our investigation shows that high values of DGD require testing with high values of SOPMD.

In this paper, we follow a standard definition of PMD

$$\vec{\tau} = \tau \cdot \hat{p} \tag{1}$$

where PMD vector $\vec{\tau}$ has length τ equal to the DGD and direction $\hat{p}$, corresponding to the principal state of polarization (PSP). Differentiating (1) with respect to frequency gives two components of SOPMD

$$\vec{\tau}_\omega = \tau_\omega \cdot \hat{p} + \tau \cdot \hat{p}_\omega = \vec{\tau}_{\omega||} + \vec{\tau}_{\omega\perp}. \tag{2}$$

The component parallel to the PMD vector $\vec{\tau}_{\omega||}$ is often called polarization dependent chromatic dispersion (PCD) [3] and the orthogonal component $\vec{\tau}_{\omega\perp}$ is frequently called depolarization.

As shown in [4], the angular speed of PSP rotation $\hat{p}_\omega$ decreases with DGD τ. The assumption was made that high values of the *orthogonal* component of SOPMD $\vec{\tau}_{\omega\perp|} = \tau \cdot \hat{p}_\omega$ seldom occur when DGD is large and, therefore, SOPMD is not important for large DGD. Our results show that, although the angular speed of the PSP rotation decreases with DGD for low DGD values, the product $\tau \cdot \hat{p}_\omega$ increases almost linearly with DGD when DGD is large. Therefore, the penalty due to the uncompensated high-order PMD increases with DGD.

We investigate the statistics of both components of the SOPMD vector as functions of DGD. We demonstrate theoretically and experimentally that the root mean square (rms) of the tangential component of the SOPMD vector increases close to linear with DGD, whereas the rms of PCD does not depend on DGD.

II. Analytical Approach

To calculate the PMD effects of first and the second order, we start with the equations connecting the PMD vector $\vec{\tau}$ and the frequency derivative of the output polarization

$$\frac{d\vec{s}}{d\omega} = \vec{\tau} \times \vec{s}. \tag{3}$$

Here, we use notation $\vec{\tau}$, proposed in [3], that allows the use of the same letter for the PMD vector and its absolute value, which describes the DGD

$$\Delta\tau = |\vec{\tau}| = \sqrt{\tau_x^2 + \tau_y^2 + \tau_z^2}. \tag{4}$$

Equation (3) can be written in a matrix form, using a transmission matrix $\hat{T}$. If $\vec{s}_{\text{in}}$ is a polarization vector at the input of a

Manuscript received December 27, 2000; revised October 30, 2001.

E. Ibragimov was with YAFO Networks, Inc., Hanover, MD 21076 USA. He is now with Scintera Networks, Inc., San Jose, CA 95129 USA (e-mail: eibragimov@scinteranetworks.com).

G. Shtengel was with YAFO Networks, Inc., Hanover, MD 21076 USA. He is now with Kodeos Communications, South Plainfield, NJ 07080 USA (e-mail: f.shtengel@kodeos.com).

S. Suh was with YAFO Networks, Inc., Hanover, MD 21076 USA. He is now with Xtellus, Florham Park, NJ 07932 USA (e-mail: sam.suh@xtellus.com).

Publisher Item Identifier S 0733-8724(02)03333-9.

PMD fiber and $\vec{s}_{\rm out}$ is a polarization vector on the output of the same fiber, so that $\vec{s}_{\rm out} = \hat{T}\vec{s}_{\rm in}$, then

$$\frac{d\vec{s}_{\rm out}}{d\omega} = \frac{d\hat{T}}{d\omega}\vec{s}_{\rm in} = \hat{T}_\omega \hat{T}^{-1}\vec{s}_{\rm out}. \tag{5}$$

Here, $\hat{T}_\omega$ is the frequency derivative of $\hat{T}$ and we assume that the input polarization does not depend on the frequency; only polarized light enters the fiber. Comparing (3) and (5) shows that applying the matrix $\hat{T}_\omega\hat{T}^{-1}$ to $\vec{s}$ is equivalent to the cross product of this vector with the PMD vector $\vec{\tau}$.

Using the relation between (3) and (5), it is possible to obtain an expression for the DGD of two concatenated pieces of fiber. Let $\hat{T}_1$ and $\hat{T}_2$ be transmission matrices for two pieces of PMD fiber and $\vec{s}_{\rm in}$ and $\vec{s}_{\rm out}$ be the polarization states at the input and output. Then, $\vec{s}_{\rm out} = \hat{T}_2\hat{T}_1\vec{s}_{\rm in}$ and

$$\begin{aligned}\frac{d\vec{s}_{\rm out}}{d\omega} &= \left(\frac{d\hat{T}_2}{d\omega}\hat{T}_1 + \hat{T}_2\frac{d\hat{T}_1}{d\omega}\right)\vec{s}_{\rm in} \\ &= \left(\hat{T}_{2\omega}\hat{T}_2^{-1} + \hat{T}_2\hat{T}_{1\omega}\hat{T}_1^{-1}\hat{T}_2^{-1}\right)\vec{s}_{\rm out}.\end{aligned} \tag{6}$$

Using (3) and the relation between $\hat{T}_\omega\hat{T}^{-1}$ and the cross product with PMD vector $\vec{\tau}$, we obtain the following expression for the DGD of two concatenated pieces of fiber:

$$\vec{\tau} = \vec{\tau}_2 + \hat{T}_2\vec{\tau}_1 \tag{7}$$

where $\vec{\tau}$ is the PMD vector of concatenation of two pieces of fiber with PMD vectors $\vec{\tau}_1$ and $\vec{\tau}_2$. Squaring and averaging (7), we obtain the known formula for PMD of two pieces of concatenated fiber, $\langle\vec{\tau}^2\rangle = \langle\tau_2^2\rangle + \langle\tau_1^2\rangle$. To obtain an analogous expression for the second-order PMD, we first differentiate (7) with respect to frequency

$$\frac{d\vec{\tau}}{d\omega} = \vec{\tau}_{2\omega} + \hat{T}_2\vec{\tau}_{1\omega} + \hat{T}_{2\omega}\hat{T}_2^{-1}\left(\hat{T}_2\vec{\tau}_1\right) \tag{8}$$

and use the analogy between (3) and (5) again

$$\vec{\tau}_\omega = \vec{\tau}_{2\omega} + \hat{T}_2\vec{\tau}_{1\omega} + \vec{\tau}_2 \times \hat{T}_2\vec{\tau}_1. \tag{9}$$

Here, $\vec{\tau}_\omega$ is the SOPMD vector of two concatenated pieces of fiber, $\hat{T}_2$ is the transmission matrix of second fiber $\vec{\tau}_1$, and $\vec{\tau}_2\vec{\tau}_{1\omega}$ and $\vec{\tau}_{2\omega}$ are the first- and second-order PMD vectors of the first and second sections, respectively. Concatenation rules (7) and (9), in slightly different form, are presented in [3] and [5].

Using (9), we can now obtain the statistical dependences between the first- and second-order PMD vectors. We represent a PMD fiber as a combination of N equal sections of polarization-maintaining fiber with random polarization scattering between the sections, as shown in Fig. 1. Here, we assume that light between the consecutive sections scatters uniformly over the Poincaré sphere (random mode coupling). In simulation, we used a scattering matrix R with three uniformly distributed random parameters, similar to three Euler angles. The transmission matrix $\hat{T}$, therefore, is the following product $T = \Delta T R_{N-1}\Delta T \ldots R_2\Delta T R_1\Delta T$ where ΔT is the transmission function of one section and R_n is a random realization of the matrix R after the nth section. To obtain the

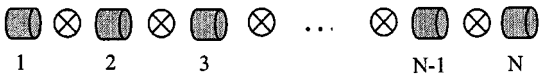

Fig. 1. The cylinders represent pieces of birefringent fiber and the crossed circles represent random polarization scattering between the sections described by the random matrix R. The random matrix R uniformly scatters polarization on the Poincare sphere. In this picture, light propagates from left to right.

expression for the second-order PMD vector for N sections, we notice that

$$\vec{\tau}_\omega \equiv \vec{\tau}_{N,\omega} = \vec{\tau}_{N-1,\omega} + \vec{\tau}_{N-1} \times \hat{T}_{N-1}\Delta\vec{\tau} \tag{10}$$

where $\Delta\vec{\tau}$ is the PMD vector of a single section and $\vec{\tau}_{N-1}$ is the PMD vector of $N-1$ concatenated sections, starting with the second and ending with the Nth section and $\hat{T}_{N-1} = \Delta T R_{N-1}\Delta T R_{N-2}\Delta T \ldots \Delta T R_1$. Notice that a single section of the birefringent fiber does not have any second-order PMD. Applying this procedure $N-1$ times, we obtain the following value for the SOPMD vector:

$$\vec{\tau}_\omega = \sum_{k=1}^{N-1} \vec{\tau}_{N-k} \times \hat{T}_{N-k}\Delta\vec{\tau}. \tag{11}$$

Here again, $\vec{\tau}_{N-k}$ is the PMD vector of $N-k$ concatenated sections starting with the kth section and $\hat{T}_{N-k} = \Delta T R_{N-1}\Delta T R_{N-2}\Delta T \ldots \Delta T R_k$.

It is easy to see that squaring and averaging of the expression (11) leads in the limit of large N to the well-known relationship between the first- and second-order PMD vectors [1]

$$\begin{aligned}\left\langle\vec{\tau}_\omega^2\right\rangle &= \Delta\tau^2 \sum_{n=1}^{N-1} \left\langle\sin^2\theta_n\right\rangle \left\langle\vec{\tau}_n^2\right\rangle \\ &= \frac{2}{3}\Delta\tau^2 \sum_{n=1}^{N-1} \left\langle\tau_n^2\right\rangle = \frac{1}{3}\left\langle\vec{\tau}^2\right\rangle^2.\end{aligned} \tag{12}$$

Here, $\Delta\tau = |\Delta\vec{\tau}|$ is the DGD of a single section and $\vec{\tau}$ is the PMD vector of the entire link. In the derivation of this expression, we assumed $\vec{\tau}_{N-k}$ and $\hat{T}_{N-k}\Delta\vec{\tau}$ to be statistically independent and θ_n to be a random angle between these vectors. As it is shown in [6], $\cos\theta_n$, in this case, will be uniformly distributed between -1 and 1.

Equation (11) is a sum of cross products of randomly oriented vectors $\hat{T}_{N-k}\Delta\vec{\tau}$ with the PMD vector of $N-k$ sections $\vec{\tau}_{N-k}$. For small k, the terms in the sum (11) are highly correlated with the vector $\vec{\tau}$ of the entire link and, therefore, the cross products $\vec{\tau}_{N-k} \times \hat{T}_{N-k}\Delta\vec{\tau}$ will be nearly perpendicular to the vector $\vec{\tau}$ for small k. The larger k is, the less correlation remains between $\vec{\tau}_{N-k}$ and $\vec{\tau}$. Within a good approximation, we can assume that all the vectors $\vec{\tau}_{N-k}$ with the numbers k smaller than a certain number K have the same magnitude and direction as $\vec{\tau}$ and all the vectors with larger numbers are completely uncorrelated with $\vec{\tau}$. In this case, the sum (11) will be divided into two parts, one proportional to $\vec{\tau}$ and another with the direction random with respect to $\vec{\tau}$

$$\vec{\tau}_\omega = \vec{c}\alpha\left|\vec{\tau}\right|\Delta\tau + \sum_{k=K+1}^{N-1} \vec{\tau}_{N-k} \times \hat{T}_{N-k}\Delta\vec{\tau} \tag{13}$$

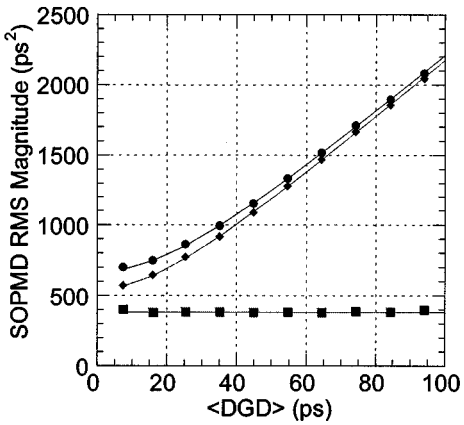

Fig. 2. Comparison of the results of numerical computations with the analytical results. Computation results: rms of full length of the full SOPMD vector (circles); rms of $\vec{\tau}_{\omega||}$ (squares); rms $\vec{\tau}_{\omega\perp}$. Solid curves are obtained using (15).

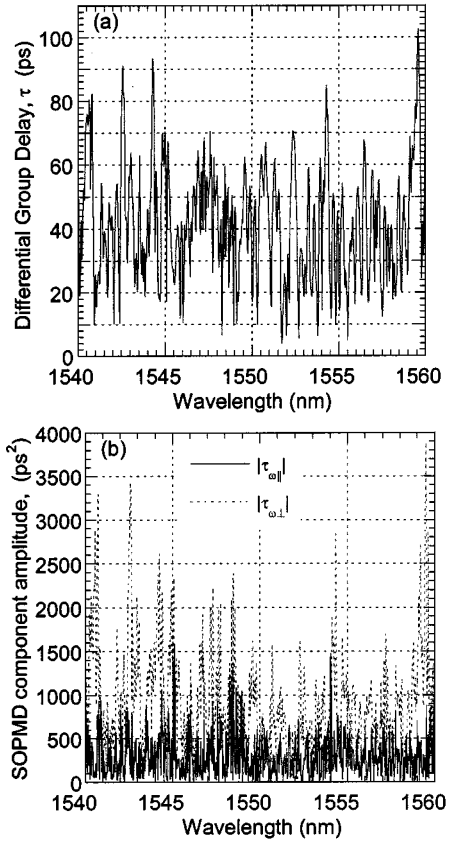

Fig. 3. Spectra of (a) the DGD and (b) two SOPMD components of the test fiber.

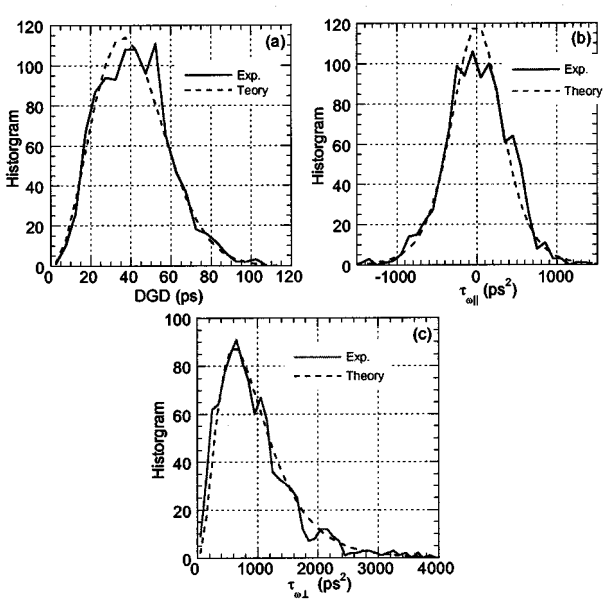

Fig. 4. Histogram of (a) DGD and SOPMD components (b) $\vec{\tau}_{\omega||}$ and (c) $\vec{\tau}_{\omega\perp}$. Solid lines are experimental data and dashed lines are theoretical curves for $\langle\tau\rangle = 41.2$ ps. Total number of samples for experimental curves is 1001.

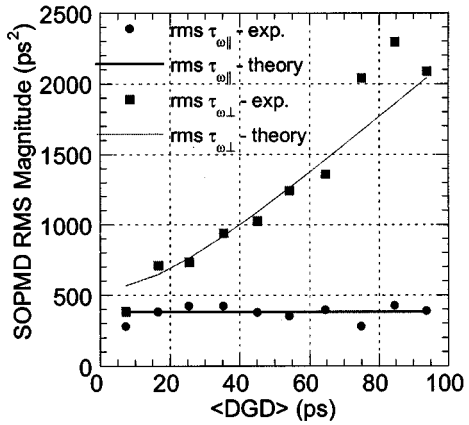

Fig. 5. Dependence of rms of $\vec{\tau}_{\omega\perp}$ (squares) and $\vec{\tau}_{\omega||}$ (circles) on $\langle$DGD$\rangle$. Solid lines are theoretical results obtained using (15).

where $\vec{c}$ is a vector perpendicular to the PMD vector of the entire link $\vec{\tau}$ and α is some coefficient. Both terms in the expression (13) are the sum of K (the first term) and $N-K$ (the second term) random vectors with length proportional to $\Delta\tau$. Therefore, the averaged mean square of $\vec{\tau}_\omega$ will scale as $\langle\tau^2\rangle$. Writing this equation for the perpendicular $\vec{\tau}_{\omega\perp}$ and parallel $\vec{\tau}_{\omega||}$ components of $\vec{\tau}_\omega$ separately, and then squaring and averaging, we obtain the following expressions for the mean squares of these components:

$$\begin{aligned}\left\langle \vec{\tau}^2_{\omega\perp}|\tau\right\rangle &= \langle\tau^2\rangle\left(F\vec{\tau}^2+P\right)\\ \left\langle \vec{\tau}^2_{\omega||}|\tau\right\rangle &= \langle\tau^2\rangle Q.\end{aligned} \tag{14}$$

Here, the sign $\langle|\tau\rangle$ denotes averaging over all states with fixed τ, while $\langle\rangle$ denotes averaging over all possible states with all possible $\vec{\tau}$. Coefficients F, P, and Q are yet to be determined.

To find the values of the coefficients in (14), we first consider the second (uncorrelated) term in the right-hand side of (13). Based on our assumptions, $\vec{\tau}_n$ in the product under the sum (13) is not correlated with $\vec{\tau}$ if $k > K$. Therefore, the value $\left\langle \vec{\tau}^2_{\omega||}\right\rangle$ of the parallel component will not depend on τ, as it is reflected in (14). This is in agreement with [2], where the probability density function of $\vec{\tau}_{\omega||}$ was shown not to depend on DGD. Because of

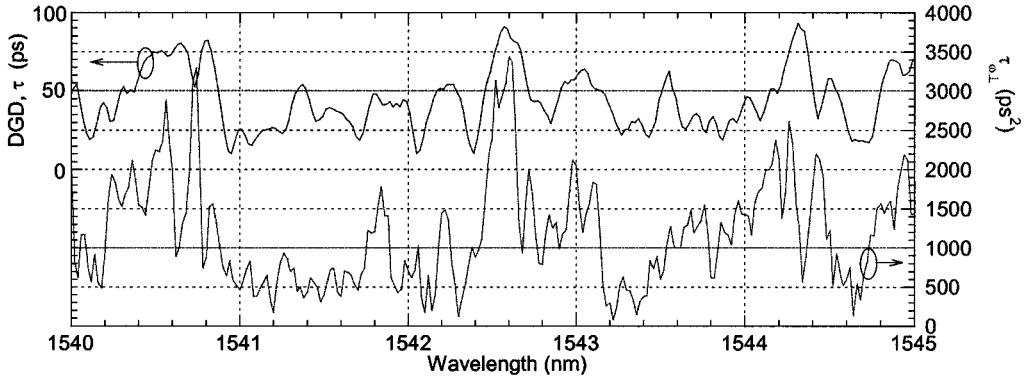

Fig. 6. τ and $\vec{\tau}_{\omega\perp}$ as functions of wavelength in a narrow range (data from the Fig. 3).

this fact, the average PCD with fixed τ is the same as the average PCD including all possible τ, $\left\langle \vec{\tau}^2_{\omega||}|\tau \right\rangle = \left\langle \vec{\tau}^2_{\omega||} \right\rangle$. Therefore, we can use a known relationship for the PCD in [2] and we obtain $Q = 1/27\langle\vec{\tau}^2\rangle$. At the same time, $\hat{T}_{N-k}\Delta\vec{\tau}$ is a random vector uniformly distributed on the Poincaré sphere. Therefore, products in (13) are also uniformly distributed and rms of the components parallel and perpendicular to the PMD vector will relate as 1 to $\sqrt{2}$. This means that $P = 2Q = 2/27\langle\vec{\tau}^2\rangle$. To find the coefficient F, we can use (12) and known values for Q and P. After squaring (13) and integrating over τ, we obtain the following expressions for rms of $\vec{\tau}_{\omega||}$ and $\vec{\tau}_{\omega\perp}$:

$$\sqrt{\langle\vec{\tau}^2_{\omega\perp}|\tau\rangle} = \frac{\sqrt{2}}{3}\sqrt{\langle\vec{\tau}^2\rangle\tau^2 + \frac{1}{3}\langle\vec{\tau}^2\rangle^2}$$
$$\sqrt{\left\langle\vec{\tau}^2_{\omega||}|\tau\right\rangle} = \frac{1}{\sqrt{27}}\langle\vec{\tau}^2\rangle. \tag{15}$$

Fig. 2 shows excellent agreement between numerical calculations obtained by random polarization scattering between sections and the analytical formulas (15). We used $125\cdot10^3$ different fibers with 2000 sections each. The DGD of a single section was 1 ps, making the average DGD equal to 41.2 ps.

III. Experimental Results

The fiber used in the experiment consisted of 12 km of old high-PMD dispersion-compensating fiber followed by 50 km of standard single-mode fiber (SMF) 28 fiber to compensate for most of the chromatic dispersion (CD). The total CD of the test fiber was measured to be -250 ps/nm. The total PDL of the test fiber is about 0.5 dB and is attributed to the DCF part, rather than to the connectors, which was confirmed by a separate measurement.

We measured DGD and PSP as functions of wavelength using both mode-matching method (MMM) [7] and Jones matrix eigenanalysis (JME) [8] methods. The measurements were performed in the wavelength range from 1540 to 1560 nm with a wavelength step 0.02 nm, yielding 1001 measurement points. No interleaving was used.

We used the three-launch JME method instead of two-launch MMM method to account for PDL. In the presence of PDL, the transmission matrix $\hat{T}$ is not unitary and, according to the Jones theorem, can be represented as a product of unitary matrix U and Hermitian matrix H, containing the PDL information [9]

$$\hat{T} = c\hat{U}\hat{H} \tag{16}$$

where c is an arbitrary complex constant. At least three independent polarization launches are required to determine the matrix T. Once the matrix $\hat{T}$ is determined, one can obtain the unitary matrix $\hat{U}$ [10]. Having characterized the dependence of the matrix $\hat{U}$ on the wavelength (optical frequency), we can use classical JME to determine the PMD vector. Poole and Wagner [11] (see also [3] for the detailed review) considered the matrix $\hat{M}$

$$\hat{M} = j\hat{U}_\omega\hat{U}^+ = j\hat{U}_\omega\hat{U}^{-1} \tag{17}$$

where dagger denotes the Hermitian conjugate. It was demonstrated that the eigenvalues of the matrix $\hat{M}$ are equal to $\pm\tau/2$ and yield the DGD value, whereas the eigenvectors are the PSP vectors. Using the measured values of DGD and PSP, we determined the values of both $\vec{\tau}_{\omega||}$ and $\vec{\tau}_{\omega\perp}$.

The measurement results are presented in Fig. 3. Shown in Fig. 3(a) is the dependence of the DGD on wavelength and in Fig. 3(b) are the spectra of $\vec{\tau}_{\omega||}$ and $\vec{\tau}_{\omega\perp}$. It is clearly noticeable from Fig. 3(b) that the magnitude of $\vec{\tau}_{\omega\perp}$ is generally much greater that that of $\vec{\tau}_{\omega||}$, according to the previous observations. Also noticeable is a correlation between the peaks of DGD and the peaks of $\vec{\tau}_{\omega||}$; see more details in Fig. 6.

Shown in Fig. 4(a) is a histogram of the DGD. The histograms of the PCD component $\vec{\tau}_{\omega||}$ and absolute value of the perpendicular component $\vec{\tau}_{\omega\perp}$ are presented in Fig. 4(b) and (c). The analytical curves were calculated directly from the theoretical model [2] using the value of $\langle\tau\rangle = 41.2$ ps obtained from the DGD measurements.

The main result of our investigation is shown in Fig. 5. It represents the statistical dependence of the parallel $\vec{\tau}_{\omega||}$ and perpendicular $\vec{\tau}_{\omega\perp}$ components of the second-order PMD vector on DGD. We averaged the DGD values within 10-ps size bins and calculated corresponding rms for $\vec{\tau}_{\omega||}$ and $\vec{\tau}_{\omega\perp}$ in the same bins. Overall, we used 1000 experimental points. Surprisingly, the two components of the second-order vector have very different behaviors with respect to the DGD in the line. The rms of $\vec{\tau}_{\omega||}$ does not depend on DGD, whereas $\vec{\tau}_{\omega\perp}$ for large DGD increases linearly. The deviation of the experiment from the theory

for the large and small DGD values we attribute to insufficient statistics in the tails of Maxwellian distribution.

It is also interesting to look into the details of the dependence of τ and $\vec{\tau}_{\omega\perp}$ on wavelength. Part of the data in Fig. 3 is presented in Fig. 6 to show the details. Again, the general correlation, described previously, shows up clearly; there are three large peaks in the spectrum of τ and there are groups of peaks in the spectrum of $\vec{\tau}_{\omega\perp}$, corresponding to each DGD peak. However the exact locations of the peaks of $\vec{\tau}_{\omega\perp}$ do not correspond to the DGD peaks exactly.

IV. Conclusion

We determined the statistical correlation between first- and second-order PMD effects. We found that the two components of the SOPMD vector behave very differently with respect to DGD (magnitude of PMD vector). In contrast to the previous suggestion that the value of the tangential component of SOPMD $\vec{\tau}_{\omega\perp}$ decreases with increasing DGD [4], we found that the rms value of $\vec{\tau}_{\omega\perp}$ increases nearly linearly with DGD. We measured the PMD spectrum of a real fiber and determined both SOPMD components. Experimental data and numerical simulations using the model consisting of 2000 randomly coupled birefringent sections are in excellent agreement with theory.

Our investigation shows the importance of the second-order and higher order PMD effects at high values of DGD; therefore, the problem of mitigating PMD at high DGD levels is increasingly complicated.

Acknowledgment

The authors wish to thank the reviewers for careful consideration and correcting inaccuracies in the original manuscript.

References

[1] G. J. Foschini, R. M. Jopson, L. E. Nelson, and H. Kogelnik, "The statistics of PMD-induced chromatic fiber dispersion," *J. Lightwave Technol.*, vol. 17, pp. 1560–1565, Sept. 1999.

[2] G. J. Foschini, L. E. Nelson, R. M. Jopson, and H. Kogelnik, "Probability densities of second-order polarization mode dispersion including polarization dependent chromatic fiber dispersion," *IEEE Photon. Technol. Lett.*, vol. 12, pp. 293–295, Mar. 2000.

[3] J. P. Gordon and H. Kogelnik, "PMD fundamentals: Polarization mode dispersion in optical fibers," *PNAS Reviews*, vol. 97, pp. 4541–4550, Apr. 2000.

[4] D. Penninckx and F. Bruyère, "Impact of the statistics of second-order polarization-mode dipersion on system performance," in *Proc. OFC'98*, Dallas, TX, Mar. 1998, ThR2, pp. 340–342.

[5] M. Karlsson and J. Brentel, "Autocorrelation function of the polarization-mode dispersion vector," *Opt. Lett.*, vol. 15, pp. 939–941, 1999.

[6] G. D. Poole and D. L. Favin, "Polarization-mode dispersion measurements based on transmission spectra through a polarizer," *J. Lightwave Technol.*, vol. 12, pp. 917–929, June 1994.

[7] R. M. Jopson, L. E. Nelson, and H. Kogelnik, "Measurement of second-order polarization-mode dispesion vectors in optical fibers," *IEEE Photon. Technol. Lett.*, vol. 11, no. 9, pp. 1153–1155, Sept. 1999.

[8] B. L. Heffner, "Automated measurement of polarization mode dispersion using Jones Matrix Eigenanalysis," *IEEE Photon. Technol. Lett.*, vol. 4, pp. 1066–1069, Sept. 1992.

[9] H. Hurwitz Jr. and R. C. Jones, "A new calculus for the treatment of optical systems. Ii: Proof of three general equivalence theorems," *J. Opt. Soc. Amer.*, vol. 31, pp. 493–499, 1941.

[10] M. Karlsson, J. Brentel, and P. Andrekson, "Long-term measurement of PMD and polarization drift in installed fibers," *J. Lightwave Technol.*, vol. 18, pp. 941–951, July 2000.

[11] C. D. Poole and R. E. Wagner, "Phenomenological approach to polarization dispersion in long single-mode fibers," *Electron. Lett.*, vol. 22, pp. 1029–1030, Sept. 1986.

E. Ibragimov (M'00) received the B.E. and M.S. degrees from Tashkent State University, Tashkent, Uzbekistan, and the Ph.D. degree from the Institute of Electronics, Tashkent.

He was formerly a Senior Research Scientist at the Institute of Electronics, and he held positions at Michigan Technological University, Houghton, MI, and University of Maryland Baltimore County, Baltimore, MD. In 2000, he joined YAFO Networks, Inc., Hanover, MD. His current position is Staff Engineer with Scintera Networks. He has extensive research and development experience in industry and academia. His research interests are in optical communications, electromagnetic theory, and wave propagation in nonlinear media.

G. Shtengel (M'94) was born in Novosibirsk, Russia. He received the M.Sc. degree in physics from St. Petersburg State Technical University, St. Petersburg, Russia, and the Ph.D. degree in physics from Stevens Institute of Technology, Hoboken, NJ, in 1996.

In 1991, he joined A. F. Ioffe Physical-Technical Institute, where he worked on high-speed modulation techniques from AlGaAs lasers. In 1993, he was a Visiting Researcher at Colorado State University, Fort Collins, where he worked on vertical cavity surface emitting lasers. In 1994, he joined Bell Laboratories (now Lucent Technologies). While at Bell Laboratories, he worked on the design of semiconductor devices (lasers, modulators, and receivers) and other wavelength division multiplexing components for fiber telecommunication systems. In 2000, he joined a startup company, YAFO Networks, Inc., Hanover, MD, where he worked on polarization mode dispersion compensation. In February 2001, he joined Kodeos Communications. He has coauthored more than 40 papers and conference presentations, and holds five patents.

S. Suh (M'99), photograph and biography not available at the time of publication.